JOURNAL OF CATALYSIS 74, 343–360 (1982)

Catalytic Synthesis of Methanol from CO/H_2

IV. The Effects of Carbon Dioxide

K. KLIER, V. CHATIKAVANIJ, R. G. HERMAN, AND G. W. SIMMONS

Department of Chemistry and Center for Surface and Coatings Research, Lehigh University, Bethlehem, Pennsylvania 18015

Received June 22, 1981

The effects of carbon dioxide on the catalytic synthesis of methanol over the copper–zinc oxide catalysts were investigated for $CO_2/CO/H_2$ ratios between 0/30/70 and 30/0/70. A maximum synthesis rate was observed at $CO_2/CO/H_2$ = 2/28/70. At lower concentrations of CO_2 the catalyst is deactivated by overreduction and at higher concentrations of CO_2 the synthesis is retarded by a strong adsorption of this gas. A kinetic model is presented which quantitatively describes the observed patterns in the indicated range of synthesis gas compositions and at temperatures between 225 and 250°C. This model is consistent with all physical characteristics of the Cu/ZnO catalysts and corroborates earlier findings that an intermediate oxidation state of the catalyst is its active state. The adsorption enthalpies and entropies for the reactants indicate that carbon dioxide is strongly bound and immobile while carbon monoxide and hydrogen are chemisorbed with intermediate strength and experience a considerable mobility in the adsorbed layer. At concentrations of CO_2 greater than 10%, methane is a side product. Mechanistic implications of this finding are that there is a nonselective pathway parallel to the CO hydrogenation; this pathway may involve formate and methoxy intermediates.

INTRODUCTION (*1*)

Carbon dioxide in small concentrations acts as a promoter of methanol synthesis from carbon monoxide and hydrogen over the low-pressure copper-based catalysts (*2*, *3*). This effect was attributed to the ability of CO_2 to keep the catalyst in its intermediate oxidation state rather than to the reversal of the Boudouart reaction

$$2CO \rightleftarrows CO_2 + C \qquad (1)$$

primarily because very little carbon was found on the surface of catalysts used with varying ratios of CO/CO_2 in the synthesis gas (*4*). It is demonstrated in this paper that small concentrations of CO_2 have a true promotion effeet on the synthesis rate rather than increasing it by direct hydrogenation of carbon dioxide to methanol that would be faster than the hydrogenation of carbon monoxide. It is established that methanol yield decreases substantially upon completely replacing carbon monoxide in the ternary syngas by carbon dioxide or by inert gas. Hence, a gradual replacement of carbon monoxide by carbon dioxide produces a maximum of the synthesis rate: at low concentrations, CO_2 acts as a promoter and at high concentrations, as a retardant of the synthesis. Such an influence of the CO/CO_2 ratio on the synthesis is of both fundamental and practical interest as it allows the catalyst to be optimized for various compositions of the synthesis gas.

In addition to mechanistic elucidation of the effects of carbon dioxide, it is desirable to formulate a kinetic equation that describes these effects quantitatively and contains temperature-dependent factors that allow the concentration and temperature distribution in industrial reactors to be predicted. Such equations were formulated before but none describes satisfactorily the synthesis patterns over the copper-based catalysts. The early kinetic equations for the high-pressure $ZnO-Cr_2O_3$ catalyst did

0021-9517/82/040343-18$02.00/0

not contain a CO_2-dependent term at all, perhaps because the effects of CO_2 were not that significant when zinc chromite catalysts are used; Natta (5) proposed the rate equation for the $ZnO-Cr_2O_3$ catalyst at temperatures 300–360°C as follows:

$$r = \frac{\gamma_{CO} p_{CO} \gamma_{H_2}{}^2 p_{H_2}{}^2 - \gamma_{CH_3OH} p_{CH_3OH}/K_{eq}}{(A + B\gamma_{CO} p_{CO} + C\gamma_{H_2} p_{H_2} + D\gamma_{CH_3OH} p_{CH_3OH})^3}, \quad (2)$$

where r is the rate of methanol synthesis, γ_i is the fugacity coefficient of species i, p_i is the partial pressure of species i, K_{eq} is the equilibrium constant of carbon monoxide hydrogenation to methanol, and A, B, C, D are empirical constants. This equation was derived under the assumption that the rate-controlling step of the synthesis is the trimolecular reaction of carbon monoxide with two hydrogen molecules in the adsorbed phase. Following Natta's publication of his data and kinetic treatment, a number of empirical as well as model-derived rate equations for methanol synthesis have been proposed, some of which have demonstrated that Natta's original data could be fitted with several kinetic models. These developments were summarized by Denny and Whan (6) up to 1977.

When the synthesis was carried out with carbon dioxide-rich synthesis gas, however, the comparison of measured rates with those calculated using kinetic Eq. (2) or its modifications (7) showed a substantial disparity (8) and it was realized that carbon dioxide-dependent terms must be incorporated in order that the kinetic equations be useful for process design. This was accomplished by Bakemeier *et al.* (9) who obtained the following rate equation, once again for the $ZnO-Cr_2O_3$ catalyst:

$$r = Ae^{-E/RT} \times \frac{p_{CO}{}^n p_{H_2}{}^m [1 - p_{CH_3OH}/(p_{CO} p_{H_2}{}^2 K_{eq})]}{(1 + De^{F/RT} p_{CO_2}/p_{H_2})} \quad (3)$$

In this equation, the quantities A, E, n, m, D, and F are semiempirical parameters. It can be seen that this rate equation predicts that the methanol yield would decrease as the CO_2 partial pressure is increased, and would drop to zero for synthesis gas that contains carbon dioxide only. Hence Eq. (3) describes a process in which carbon dioxide is a retardant but not at all a reactant.

In 1973, Leonov *et al.* (10) put forward a kinetic rate equation for the low-pressure copper–zinc oxide–alumina catalyst for temperatures between 220 and 260°C. The rate equation was proposed to be:

$$r = k\left[\frac{p_{CO}^{0.5} p_{H_2}}{p_{CH_3OH}^{0.66}} - \frac{p_{CH_3OH}^{0.34}}{p_{CO}^{0.5} p_{H_2} K_{eq}}\right], \quad (4)$$

where k is the rate constant for the forward reaction, and K_{eq} is the equilibrium constant. Similar to the early kinetic studies with the high-pressure $ZnO-Cr_2O_3$ catalysts, there are no CO_2-dependent terms in Eq. (4) for the low-pressure synthesis.

Denny and Whan (6) also reviewed various contrasting reports on the effects of CO_2 on the synthesis, and emphasized that any complete kinetic expression should include a term involving the partial pressure of carbon dioxide. A rate equation that does contain an empirical CO_2-dependent term for the Cu–ZnO–alumina catalysts has been presented in 1980 by Andrew (3) in the form

$$r = k\, p_{H_2}^{0.7}\, p_{CO}^{0.2 \text{ to } 0.6} \Phi_{CO_2}. \quad (5)$$

Although the function Φ_{CO_2} was not explicitly determined, it was reported that the rate of methanol synthesis reached a maximum at the CO_2 to CO partial pressure ratio around 0.01, and decreased as the CO_2 pressure was further increased. It was also indicated that the methanol synthesis rate would decline at very small concentrations of CO_2. A behavior like this was also reported to be the property of the binary Cu–

ZnO catalysts (*2*), and hence it seems established that an optimum concentration of CO_2, or a ratio of CO_2 and CO concentrations, exists at which the low pressure synthesis runs at its maximum rate.

We have undertaken a study to determine which mechanistic, kinetic, and thermodynamic phenomena will give rise to a maximum synthesis rate at a certain concentration of carbon dioxide. In the process of doing so, we were able to formulate models, presented in this work, that quantitatively interpret the observed rates for various compositions of the synthesis gas. Thermodynamic functions derived from the comparison of the model-based kinetic equations with experiment give insight into the role of redox equilibria and competitive adsorption of reactants in determining the synthesis rate at a given CO_2/CO ratio and temperature. It is possible that these data and theory will lead to a further development of catalysts for synthesis gases of various composition and origin. While this may be a beneficial effort in most instances, its applicability may be limited in those cases where methanol synthesis is accompanied by that of side products. For this reason we also present data on the dependence of the catalyst selectivity on the pressure of carbon dioxide. We have focused on a single catalyst of the composition Cu/ZnO = 30/70, described and characterized in our earlier work (*2*, *11*, *12*), because this catalyst operates in a well-defined structural, morphologic, and electronic state while retaining high activity and selectivity to methanol.

EXPERIMENTAL

Activity and selectivity tests. The catalysts of composition Cu/ZnO = 30/70 metal atomic percent were tested in a flow reactor described previously (*2*) at a pressure of 75 atmospheres, temperatures of 225, 235, and 250°C, synthesis gas hourly space velocity of about 6100 liters/kg catalyst/hr, and varying ratios of concentrations of CO_2 to CO in mixtures containing carbon to molecular hydrogen mole ratio of 30/70. Gas mixtures CO_2/CO/H_2 = 0/30/70, 2/28/70, 4/26/70, 6/24/70, 8/22/70, 10/20/70, 20/10/70, and 30/0/70 were used. Additional tests were made with CO_2/Ar/H_2 = 6/24/70 and Ar/CO/H_2 = 6/24/70. All gases in this work were high purity and were obtained, either pure or premixed to desired compositions, from Air Products and Chemicals. The product gas from the reactor was sampled every 7 to 15 min using an automated sampling valve and analyzed using an online Hewlett–Packard 5730A gas chromatograph, coupled with a Model 3388A integrator, equipped with a Porapak Q column for separation of CO, CO_2, CH_4, CH_3OH, and H_2O. Dimethyl ether was not a product in our series of experiments. A thermal conductivity detector was used for quantitative analyses of the products with sensitivity factors of 42 for CO, 37.5 for CH_4, 48 for CO_2, 33 for H_2O, and 45 for CH_3OH. All except the methanol sensitivity factor agree with those in Ref. (*13*). The methanol factor was determined by measuring the TC gauge response to samples from a helium stream saturated by methanol at different temperatures and from the oxygen balance in the synthesis. The results of both methods agree and yield the sensitivity factor 45 for methanol. Integrated areas divided by the sensitivity factors were normalized to give the molar fractions of the gas products. Prior to testing, each catalyst was reduced in flowing 2% H_2 in N_2 at ambient pressure (3.5 liters/hr). The temperature was increased at about 3.5°C/min to 250°C, and reduction was initiated at approximately 210°C. The treatment was maintained until the evolution of water stopped, as shown by gas chromatography analyses. After each activity test, the catalyst was removed from the reactor in a nitrogen-filled glove bag and stored in nitrogen for X-ray diffraction and surface area measurements.

Catalyst preparation. The catalysts were coprecipitated from a (Cu,Zn) nitrate solution by sodium carbonate, calcined, and re-

duced according to a procedure described in detail earlier (*2*). Each tested sample contained 2.45 g of calcined CuO/ZnO catalyst of molar ratio CuO/ZnO close to 30/70. These samples were taken from four batches: 1 (exact composition CuO/ZnO = 30.23/69.77), 2 (exact composition CuO/ZnO = 29.76/70.24), 3 (nominal composition = 30/70), and 4 (nominal composition = 30/70).

Catalyst characterization. Surface area determinations and X-ray diffraction were carried out using instruments and methods referenced in our earlier work (*2*). The particle sizes were determined from the diffraction peak half-widths using the Scherrer equation (*14*) for the Cu(111) and Cu(200) reflections at $2\theta = 43.2°$ and 50.4°, respectively, and for the ZnO(101) and ZnO(110) reflections at $2\theta = 36.5$ and 56.6°, respectively. The instrumental half-width was 0.2°.

RESULTS

Effects of CO_2 on Methanol Synthesis at Steady State

The activities of the Cu/ZnO = 30/70 catalysts were tested at three temperatures of 250, 235, and 225°C. Steady conversions were reached within 1–20 hr after establishing the p, T, GHSV, and feed gas composition, and for all except CO_2-free synthesis gas could be maintained for weeks. The observed steady state conversions and conditions are summarized in Table 1, together with the designations for each of the four batches of catalyst and for the samples that were tested.

Each catalyst sample denoted by a separate identification number was taken from a calcined batch 1 to 4, as noted, charged into the reactor, reduced, and tested under the specified conditions. Hence, the spread of conversion rates for a given set of conditions encompasses all preparation and testing variables. Eight tests were carried out with the $CO_2/CO/H_2$ = 6/24/70 synthesis gas, and the measured conversions indicate an accumulated relative experimental error of ±7%. Our earlier testing results (*2*) are well within this margin.

The synthesis pattern in Table 1 demonstrates that there is indeed a maximum on the dependence of methanol synthesis rate vs the CO_2/CO ratio in the synthesis gas, which appears where CO_2 and CO are simultaneously present and not when either of these two gases is replaced by inert argon. An additional finding of significance is that selectivity changes with the synthesis gas composition. At concentrations of CO_2 between 0 and 10%, methanol is the sole product while at higher concentrations of CO_2 methane is formed as a side product. The highest rate of methane production was obtained at the lowest investigated temperature, a behavior that has mechanistic implications as will be discussed below. Dimethyl ether was not found at any of the conditions investigated using the present catalyst.

Transient Effects

All the catalysts tested with a feed gas with a given CO_2 content were found to attain a new steady-state activity when another concentration of CO_2 was used in the synthesis gas. The final steady-state conversions were the same as those listed in Table 1 for catalysts freshly exposed to the synthesis gas of the given composition. However, the duration of time necessary to attain a new steady state after a change of synthesis gas composition depended on the previous history of the catalyst exposure to the gas mixtures. Between the compositions $CO_2/CO/H_2$ = 2/28/70 and 20/10/70, the methanol conversion rates rapidly responded to the changes of CO_2/CO concentration ratio. This behavior is illustrated in Fig. 1 which depicts the time development of CO, CO_2, CH_3OH, and H_2O concentrations after a switch from $CO_2/CO/H_2$ = 20/10/70 to 6/24/70 gas mixture. The new steady state was established within 30 min.

TABLE 1

Conversions of Synthesis Gas to Methanol and Methane over Reduced Cu/ZnO Catalysts

Gas composition $CO_2/CO/H_2$ (vol%)	Temperature (°C)	Percentage carbon conversion to		Catalyst batch No.	Sample No.
		CH_3OH	CH_4		
0/30/70	225	4.9	0	1	5
	235	8.8	0		
	250	11.0, 12.1[a]	0		
	250	14.5, 10.8[b]	0	1	11
2/28/70	225	36.5	0	1	4
	235	50.7	0		
	250	69.7, 68.3[a]	0		
	250	68.3	0	1	8
	250	67.6	0	2	13
	250	69.8	0	4	15
4/26/70	225	19.6	0	1	2
	235	33.1	0		
	250	56.5	0		
	250	51.5	0	1	8
6/24/70	225	18.2	0	1	1
	235	33.5	0		
	250	57.8, 59.2[a]	0		
	235	37.3	0	4	16
	250	54.7, 54.4[b]	0	1	2
6/24/70	250	55.1	0	1	3
	250	53.8	0	1	9
	250	60.9, 56.5[b]	0	1	11
	250	58.2	0	2	12
	250	51.1[c]	0	3	14
	250	51.9	0	4	15
8/22/70	225	17.7	0	1	7
	235	33.4	0		
	250	54.4	0		
10/20/70	225	11.9	0	4	16
	235	26.5	0		
	250	40.5	0		
	250	43.1, 45.1[a]	0	1	6
20/10/70	225	8.0	2.8	1	9
	235	12.0	2.6		
	250	22.6, 22.5[a]	2.3, 2.5[a]		
30/0/70	225	6.5	4.1	1	1
	235	7.4	3.5		
	250	9.7	2.5		
	225	6.4	2.6	1	10
	235	7.4	2.5		
	250	10.0	2.3		
$CO_2/Ar/H_2$ = 6/24/70	250	3.0[e]	1.5[e]	4	15
$Ar/CO/H_2$ = 6/24/70[d]	250	12.2[e]	0	4	15

[a] Catalytic activities at 225 and 235°C were obtained between the 250°C determinations.

[b] Catalytic testing was carried out at this temperature with other synthesis gas mixtures being utilized between these determinations.

[c] From Ref. (*2*).

[d] Actual synthesis gas composition was approximately $CO_2/Ar/CO/H_2$ = 0.09/6/24/70 vol %.

[e] For the sake of comparison with other entries in this table, conversions in the presence of argon are given as percent of $CO_2 + CH_3OH + CH_4 + Ar$ or $CO + CH_3OH + CH_4 + Ar$.

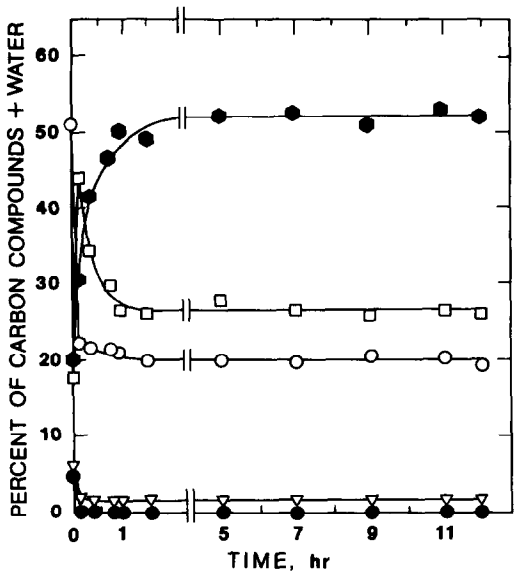

FIG. 1. The effect of changing the synthesis gas composition from $CO_2/CO/H_2$ = 20/10/70 to $CO_2/CO/H_2$ = 6/24/70 after testing in the initial gas mixture for 12 hr at 250°C. The analyzed products are CO(□), CO_2(○), CH_3OH(●), H_2O(▽), and CH_4(●).

Contrary to this behavior, catalysts that were exposed to the CO_2-free synthesis gas $CO_2/CO/H_2$ = 0/30/70 recovered their activity in CO_2-containing gas only after an extended period of time; after a prolonged exposure to CO_2-free synthesis gas, the catalysts recovered their activity only partially. For example, a Cu/ZnO = 30/70 catalyst exposed to $CO_2/CO/H_2$ = 0/30/70 for 12 hr attained a steady conversion to methanol of 10.5% at 250°C; upon exposure to a new synthesis gas $CO_2/CO/H_2$ = 6/24/70, the methanol yields increased sharply, then fluctuated for several hours, and reached a new steady state at 47% conversion after 18 hr. The same catalyst freshly exposed to $CO_2/CO/H_2$ = 6/24/70 synthesis gas showed conversions between 51 and 61%, as listed in Table 1, and so the catalyst preexposed to CO_2-free synthesis gas was partially irreversibly deactivated. Such a deactivation is progressively more severe with more prolonged preexposures to CO_2-free synthesis gas.

Catalyst Characterization

X-Ray diffraction was used to determine particle sizes of the ZnO and Cu crystallites prior to and after testing. The latter results are summarized in Table 2. The ZnO(101) reflections yield larger sizes than ZnO(110) reflections because the zinc oxide crystallites have a longer dimension along the hexagonal axis [001]. The Cu particles are more isotropic and so the sizes determined from the (111) and the (200) reflections are closer to each other. Although the determination of particle sizes is burdened by a considerable error, comparison of the X-ray particle dimensions permits the conclusion that no significant changes in particle size resulted from the exposure and use of the catalyst to various synthesis gas compositions. However, BET area measurements did reveal a downward trend from about 41 to 33 m^2/g when the CO_2 gas content increased from 0 to 30 parts per hundred, as indicated in Table 3. This effect is due to filling of micropores by CO_2 and has been observed in an independent study of CO_2 chemisorption on the Cu/ZnO catalyst (*15*). The original surface area around 40 m^2g can be recovered, e.g., by heat treatment of the catalyst in vacuum.

TABLE 2

Particle Dimensions of Cu and ZnO Crystallites in the Tested Cu/ZnO = 30/70 Catalysts as Determined by X-Ray Powder Diffraction

Gas composition $CO_2/CO/H_2$ (vol%)	Particle size (nm)				Sample designation (batch–sample)
	Copper		Zinc oxide		
	(111)	(200)	(101)	(110)	
0/30/70	7.9	5.5	11.8	10.8	1–5
0/30/70[a]	6.4	6.3	17.0	15.4	1–11
2/28/70[a]	6.9	5.7	13.6	13.3	1–4
4/26/70[a]	6.2	—	14.3	13.9	1–2
6/24/70	5.5	5.7	12.3	10.5	1–1
8/22/70	6.2	5.7	14.3	13.9	1–7
10/20/70[a]	6.9	5.2	15.1	13.9	1–6
30/0/70	6.4	7.1	20.9	16.3	1–10
Estimated error	±0.2	±0.3	±0.8	±0.9	

[a] The final catalytic testing of these samples was carried out with a $CO_2/CO/H_2$ = 6/24/70 vol% synthesis gas.

TABLE 3

BET Surface Areas of the Cu/ZnO = 30/70 Catalysts Tested in Various Compositions of the Synthesis Gas

Synthesis gas composition $CO_2/CO/H_2$	BET surface area (m^2/g)	Treatment	Batch–sample
0/30/70	40.9		1–5
2/28/70	37.8	*a*	1–4
4/26/70	40.4	*a*	1–2
6/24/70	42.1		1–1
6/24/70	37.1[b]		3–14
8/22/70	37.7		1–7
10/20/70	36.8	*a*	1–6
30/0/70	33.0		1–10

[a] Final catalytic testing was carried out with $CO_2/CO/H_2$ = 6/24/70 vol% synthesis gas.
[b] From Ref. (*2*).

DISCUSSION

The increase of the methanol synthesis rate upon replacement of small amounts of CO in the CO/H_2 synthesis gas by CO_2 is a true promotion effect and not an effect ensuing from a negative power dependence of the synthesis rate upon partial pressure of CO. This is demonstrated by the low conversion obtained when all CO_2 in the $CO_2/CO/H_2$ = 6/24/70 synthesis gas was replaced by argon (Table 1). Such a promotion effect of CO_2 is not described by any of the equations (2)–(4) presented in the Introduction or in Denny's and Whan's review (*6*). Neither does hydrogenation of CO_2 account for the increase in methanol yield: at $CO_2/CO/H_2$ = 6/24/70 and at 250°C, approximately 95% of the yield of methanol is produced by hydrogenation of carbon monoxide and only about 5% by hydrogenation of CO_2.

Carbon dioxide does undergo hydrogenation but at a much lower rate than CO. This is seen from the relative consumption of CO and CO_2 where both gases are present, from the rate of hydrogenation of synthesis gas containing CO_2 and hydrogen only, and from the rates of hydrogenation of the mixture containing CO_2, argon, and hydrogen (Table 1). Although the rate of its hydrogenation is slow, carbon dioxide does become a significant source of carbon for methanol when CO_2-rich synthesis gas is used. The kinetic equations listed in the Introduction also do not account for this feature of the synthesis. It is evident that the synthesis pattern over the low-pressure–low-temperature copper-based catalysts and over the wide range of CO_2 concentrations, exemplified by the data presented in Table 1, requires a new kinetic model that will encompass all effects of CO_2 and, ultimately, provide a quantitative interpretation of the conversion rates on the CO_2 concentration. Such a model is presented in the following section.

Kinetic Model for Methanol Synthesis over the Cu/ZnO Catalysts

The kinetic model put forward here is based on observations in Table 1 and on various findings concerning the chemical and physical properties of the Cu/ZnO catalysts reported earlier or intended for communication. These findings are summarized as follows:

(1) The methanol conversion rates from the CO/H_2 synthesis gas increase substantially with the addition of CO_2 (present work), H_2O, or even small amounts of oxygen (*2*). The catalyst is irreversibly deactivated by prolonged exposure to synthesis gas containing CO and H_2 only.

(2) A catalyst that has been reduced by hydrogen at 250°C can be further reduced by CO at the same temperature with the appearance of CO_2. When this CO-reduced catalyst is exposed to CO_2, also at 250°C, it is reoxidized and CO_2 is converted to CO. The CO/CO_2 equilibria are established in a time frame of hours (*16*).

(3) The activity of the catalyst increases as a high power of the concentration of amorphous copper, which was earlier identified as a solute species in the zinc oxide phase. The catalyst activity to methanol is not proportional to nor monotonously

dependent on the surface area of crystalline copper particles that are also present in the catalyst. This latter finding has been a matter of controversy (*1*, *3*) but we have additional evidence of its correctness based on chemisorption of carbon monoxide and oxygen (*16*).

(4) Carbon dioxide is adsorbed quite strongly. The reactant adsorption strengths are estimated to decrease in the order $CO_2 > CO > H_2$.

Based on the results listed in Table 1 and on observations summarized *sub* 1–4 above, the model of the synthesis is formulated as follows:

(i) The catalyst can exist in a reduced state A_{red} and in an oxidized state A_{ox}. The oxidized state is active and the reduced state is inactive (cf. 1 above). The proportion of A_{ox} and A_{red} is controlled by the ratio of CO_2 and CO in the synthesis gas (cf. 2).

(ii) Several active centers A_{ox} are involved in each reaction step. These centers may be identified with copper solute species in zinc oxide (cf. 3).

(iii) All three components of the synthesis gas CO, H_2, and CO_2 react in the adsorbed layer. CO_2 competes for active sites with at least one of the reactants CO and H_2. The adsorption strengths are in the order $CO_2 > CO > H_2$ (cf. 4).

(iv) The products CH_3OH, H_2O, and CH_4 are adsorbed weakly; their effect on the reaction rate is taken into consideration by kinetic terms for the reverse reaction but not for product desorption in the forward reaction.

The model outlined in statements (i)–(iv) satisfactorily explains, unlike many other models considered earlier, the data in Table 1 and is general enough to accommodate changes of the catalyst caused by exposure to different synthesis gas compositions. In particular, the equilibrium

$$A_{red} + CO_{2(g)} \rightleftharpoons A_{ox} + CO_{(g)} \qquad (6)$$

summarily involves redox equilibria between valence states of copper and zinc in zinc oxide and electron equilibria between the various accessible energy bands.

A specific mathematical treatment that results in quantitative interpretation of our data is presented hereafter:

Ad(i): Take the redox equilibrium (6) to be established in the adsorbate with equilibrium constant K'. The requirement that the reduced and oxidized forms of the catalyst sum up to a constant, $A_0 = A_{red} + A_{ox}$, yields for the concentration of active centers

$$A_{ox} = A_0 \frac{K'(p_{CO_2}/p_{CO})}{1 + K'(p_{CO_2}/p_{CO})} \qquad (7)$$

Ad(ii): The forward reaction rate r is assumed to be determined by the rate of the surface reaction involving one CO and two H_2 molecules to produce methanol plus the empirical term $k'p_{CO_2}$ for the slow hydrogenation of CO_2,

$$r = k(A_{ox}\theta_{CO})(A_{ox}\theta_{H_2})^2 + k'p_{CO_2}, \qquad (8)$$

where θ_{CO} and θ_{H_2} are fractions of the active surface A_{ox} occupied by CO and H_2, respectively. The surface concentrations of each reacting species are $A_{ox}\theta_{CO}$ and $A_{ox}\theta_{H_2}$, respectively. The linear dependence $k'p_{CO_2}$ of the rate r_{CO_2} of CO_2 hydrogenation on the pressure of CO_2 follows from the comparison of carbon conversions of synthesis gases $CO_2/CO/H_2 = 30/0/70$ and $CO_2/Ar/H_2 = 6/24/70$ given in Table 1, also shown in Fig. 2 and connected by a dotted line representing $r_{CO_2} = k'p_{CO_2}$.

Ad(iii): Surface equilibria

$$CO_{(g)} \underset{K_{CO}}{\rightleftharpoons} CO_{(a)}$$

$$CO_{2(g)} \underset{K_{CO_2}}{\rightleftharpoons} CO_{2(a)}$$

$$H_{2(g)} \underset{K_{H_2}}{\rightleftharpoons} H_{2(a)}$$

are rapidly established, as determined from adsorption measurements, and are assumed to obey Langmuir isotherms. Three cases will be examined here, one in which CO, CO_2, and H_2 compete for the same sites (Case I), another in which CO and H_2 are adsorbed on different sites and CO_2 competes for the hydrogen sites (Case II), and a case wherein CO_2 competes for both the CO sites and the hydrogen sites (Case III). The corresponding Langmuir isotherms are as follows:

Case I

$$\theta_i = \frac{K_i p_i}{(1 + K_{CO}p_{CO} + K_{CO_2}p_{CO_2} + K_{H_2}p_{H_2})}, \tag{9}$$

where the subscript i stands for CO, CO_2, or H_2.

Case II

$$\theta_{CO} = \frac{K_{CO}p_{CO}}{(1 + K_{CO}p_{CO})} \tag{10}$$

$$\theta_{H_2} = \frac{K_{H_2}p_{H_2}}{(1 + K_{H_2}p_{H_2} + K_{CO_2}p_{CO_2})} \tag{11}$$

Case III

$$\theta_{CO} = \frac{K_{CO}p_{CO}}{(1 + K_{CO}p_{CO} + K_{CO_2}p_{CO_2})} \tag{12}$$

$$\theta_{H_2} = \frac{K_{H_2}p_{H_2}}{(1 + K_{H_2}p_{H_2} + K_{CO_2}p_{CO_2})} \tag{13}$$

Ad(iv): Combining (7), (8), and (9) and replacing $p_{CO}p_{H_2}^2$ by $p_{CO}p_{H_2}^2 - p_{MeOH}/K_{eq}$ and p_{CO_2} by $p_{CO_2} - p_{MeOH}p_{H_2O}/p_{H_2}^3/K'_{eq}$ to account for the reverse reactions, we obtain for Case I

$$r = kA_0^3 \frac{K'^3\left(\frac{p_{CO_2}}{p_{CO}}\right)^3}{\left[1 + K'\left(\frac{p_{CO_2}}{p_{CO}}\right)\right]^3} \cdot \frac{K_{CO}K_{H_2}^2(p_{CO}p_{H_2}^2 - p_{MeOH}/K_{eq})}{(1 + K_{CO}p_{CO} + K_{CO_2}p_{CO_2} + K_{H_2}p_{H_2})^3}$$

$$+ k'\left(p_{CO_2} - \frac{1}{K'_{eq}}\frac{p_{MeOH}p_{H_2O}}{p_{H_2}^3}\right) \tag{14}$$

where K_{eq} is the equilibrium constant of the reaction

$$CO_{(g)} + 2H_{2(g)} \underset{K_{eq}}{\rightleftharpoons} CH_3OH_{(g)} \tag{15}$$

and K'_{eq} is the equilibrium constant of the reaction

$$CO_{2(g)} + 3H_{2(g)} \underset{K'_{eq}}{\rightleftharpoons} CH_3OH_{(g)} + H_2O_{(g)}. \tag{16}$$

The definitions of K_{eq} and K'_{eq} involving fugacities and their numerical values are given in Appendix I. Under all reaction conditions employed here the term with $1/K'_{eq}$ for reverse reaction (16) is negligible.

Equation (14) for the overall rate has the

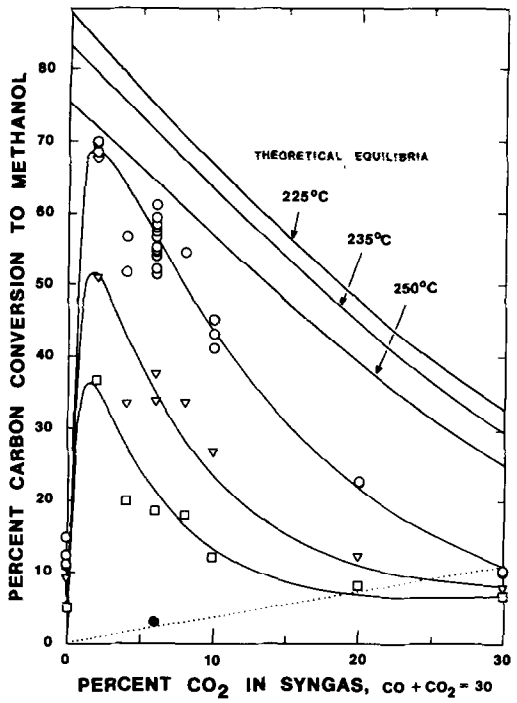

FIG. 2. The dependence of carbon conversion to methanol in a $CO_2/CO/H_2$ synthesis gas containing 70% H_2 and a variable ratio of CO_2 and CO. Experimental data are shown for 250°C(○), 235°C(▽), and 225°C(□). Lines drawn through the data points are theoretical curves derived from the model described in text. Theoretical equilibrium methanol conversions for the three temperatures studied are also shown as heavy lines in the upper portions of the figure. The point ● denotes the yield in $CO_2/Ar/H_2$ = 6/24/70 synthesis gas, expressed in terms of equivalent conversion of (CO_2 + Ar) to methanol. The dotted line represents the rate of CO_2 hydrogenation $r_{CO_2} = k' p_{CO_2}$.

following features: at $p_{CO_2}/p_{CO} = 0$, the rate is zero because the oxidized active site concentration is zero [e.g., (7)]; at $p_{CO}/p_{CO_2} = 0$, the rate is given by the CO_2-only term $k' p_{CO_2}$ [e.g., (14)]; at intermediate values of p_{CO_2}/p_{CO}, there is a maximum rate, the position of which is primarily determined by the values of K' and K_{CO_2}. Thus the maximum rate is obtained at such pressures of CO_2 that are sufficient to bring the catalyst into the active state A_{ox} but are not too high to retard the synthesis by excessive CO_2 adsorption.

Equations analogous to (14) for Cases II and III are obtained by combining (7) and (8) with (10) and (11) or with (12) and (13), respectively. All these equations have a general form

$$r = \text{const}\left(1 + \frac{1}{K'}\frac{p_{CO}}{p_{CO_2}}\right)^{-3} \times \frac{(p_{CO}p_{H_2}^{\,2} - p_{MeOH}/K_{eq})}{(F + K_{CO_2}p_{CO_2})^n} + k'\left(p_{CO_2} - \frac{1}{K'_{eq}}\frac{p_{MeOH}p_{H_2O}}{p_{H_2}^{\,3}}\right) \quad (17)$$

where F is a linear function of pressures of H_2 and CO and the exponent n ranges from 1 to 3. The term with k' accounts for the relatively low direct conversion of CO_2. Equations of the type (17) adequately explain the observations of Table 1. Several other types of rate equations, including all listed in the Introduction, were found inadequate.

Rate equation (17) can be used in its integral form to calculate carbon conversion α in an integral isothermal flow reactor using

$$\alpha = \alpha_{CO} + \alpha_{CO_2} = \frac{1}{(F_{CO}^{\,0} + F_{CO_2}^{\,0})}\int_0^M r_m\, dm. \quad (18)$$

Here $F_{CO}^{\,0}$ and $F_{CO_2}^{\,0}$ are the flow rates of CO and CO_2 at the beginning of the catalyst bed of total catalyst mass M. The differential rate r_m is the rate r of Eq. (17) expressed per unit mass of the catalyst in a mass element dm at a cross-section of the catalyst bed (17). The conversions of CO and CO_2 to methanol are defined as

$$\alpha_{CO} = \frac{F_{MeOH}^{CO}}{F_{CO}^{\,0} + F_{CO_2}^{\,0}}$$

and

$$\alpha_{CO_2} = \frac{F_{MeOH}^{CO_2}}{F_{CO}^{\,0} + F_{CO_2}^{\,0}}$$

with F_{MeOH}^{CO} and $F_{MeOH}^{CO_2}$ being flow rates of methanol produced from CO and CO_2, respectively. The reaction rate r_m is a known function of α_{CO} and α_{CO_2} through the pressure terms

$$\frac{p_i}{P} = \frac{F_i(\alpha_{CO},\alpha_{CO_2})}{\sum_i F_i},$$

where P is the total pressure and the F_i terms are:

$$F_{CO} = F_{CO}^0 - \alpha_{CO}(F_{CO}^0 + F_{CO_2}^0)$$

$$F_{CO_2} = F_{CO_2}^0 - \alpha_{CO_2}(F_{CO}^0 + F_{CO_2}^0)$$

$$F_{H_2} = F_{H_2}^0 - (2\alpha_{CO} + 3\alpha_{CO_2})(F_{CO}^0 + F_{CO_2}^0)$$

$$F_{MeOH}^{CO} = \alpha_{CO}(F_{CO}^0 + F_{CO_2}^0)$$

$$F_{MeOH}^{CO_2} = F_{H_2O} = \alpha_{CO_2}(F_{CO}^0 + F_{CO_2}^0).$$

These relationships between conversion and flow rates of the reaction components hold at any cross-section of the reactor and, therefore, given that the total pressure P is constant, the partial pressures p_i and reaction rate r are determined at any m. Equation (18) can then be solved numerically by calculating the increments of conversion from

$$d\alpha_{CO} = r_{CO}\, dm/(F_{CO}^0 + F_{CO_2}^0)$$

$$d\alpha_{CO_2} = r_{CO_2}\, dm/(F_{CO}^0 + F_{CO_2}^0),$$

where r_{CO} and r_{CO_2} are the rates of methanol production by hydrogenation of CO and CO_2, respectively, given by Eq. (17) and by

$$r = r_{CO} + r_{CO_2} \quad \text{and} \quad r_{CO_2} = k' p_{CO_2}.$$

The algorithm for this procedure is briefly outlined in Appendix II.

Application of the Kinetic Model to the Evaluation of Methanol Synthesis Rate as a Function of p_{CO_2}/p_{CO}

The model described in the preceding paragraph was used for the fitting, interpretation, and determination of kinetic as well as thermodynamic constants of the synthesis from data presented in Table 1. First, the best fit was obtained for the conversion rates at 250°C by finding the optimum set of constants kA_0^3, k', K', K_{CO}, K_{CO_2}, and K_{H_2} by trial and error. A subsequent fit of the rates at 235°C was restricted by the requirement that the temperature coefficients of the equilibrium constants K_{CO}, K_{CO_2}, and K_{H_2} yield enthalpies that fall within the range of published or estimated values of adsorption heats of these gases. Finally, the theoretical curve for 225°C was calculated from values of the constants predicted from their temperature coefficients and their values at 250°C. The best set of constants is summarized in Table 4 for Cases I, II, and III. The theoretical curves for Case I are represented along with data from Table 1 in Fig. 2.

The comparison of the theoretical curves with experimental points plotted in Fig. 2 shows that our present model is very satisfactory for Case I in the whole range of temperatures and synthesis gas compositions. Cases II and III give nearly equally satisfactory fits with the values of constants listed in Table 4. It is evident that the goodness of the fit is a consequence of the general form (17) of the dependence of the synthesis rate on pressure of CO_2 and that the kinetics are not sensitive to specific features such as whether the adsorption of CO and H_2 are competitive or noncompetitive. Thus the kinetics reflect primarily the promotion by CO_2 through the creation of active sites A_{ox} and the retarding effects of CO_2 at high concentration through its adsorption.

It is interesting to examine the range of adsorption enthalpies and entropies of the reactants calculated from the constants in Table 4. The values of these thermochemical entities, summarized in Table 5, will reveal whether the kinetic model used here is sound in terms of physicochemical characteristics of adsorption, and will render the model testable by independent measurements of adsorption energies. Also given in Table 5 are activation energies for the kinetic constants k and k'.

Inspection of the data in Table 5 reveals that Cases I and III yield nearly identical sets of adsorption enthalpies and entropies, and Case II differs only in that the absolute values of adsorption enthalpies and entro-

TABLE 4

Values of Constants Used for the Construction of Theoretical Dependences of Steady-State Carbon Conversions to Methanol upon the Percentage x of CO_2 in the Synthesis Gas of Composition $CO_2/CO/H_2 = x/(30 - x)/70$[a]

Case	Temperature (°C)	K_{CO}	K_{H_2}	K_{CO_2}	K'	kA_0^{s} [b]	k' [b]	K_{eq} [c]	K'_{eq} [c]	(Σ^2/n) [d]
I	225	12.52	1.77	39.62	158.2	1.064	2.18(−4)	9.034(−3)	9.237(−5)	
	235	8.58	1.40	21.52	125.4	1.253	2.70(−4)	5.409(−3)	6.573(−5)	0.0012
	250	5.00	1.00	9.00	90.0	1.584	3.75(−4)	2.625(−3)	4.095(−5)	
II	225	12.52	1.77	98.51	18.1	0.898	2.18(−4)	9.034(−3)	9.237(−5)	
	235	8.58	1.40	60.0	16.1	1.135	2.70(−4)	5.409(−3)	6.573(−5)	0.0016
	250	5.00	1.00	30.0	13.8	1.584	3.75(−4)	2.625(−3)	4.095(−5)	
III	225	12.52	1.77	19.8	79.1	0.088	2.18(−4)	9.034(−3)	9.237(−5)	
	235	8.58	1.40	10.8	62.7	0.120	2.70(−4)	5.409(−3)	6.573(−5)	0.0015
	250	5.00	1.00	4.5	45.0	0.195	3.75(−4)	2.625(−3)	4.095(−5)	

[a] A total pressure of 75 atm was maintained at all conversions.

[b] Rate constants per gram of catalyst per hour for rates expressed in moles of methanol per hour.

[c] Equilibrium constants for reactions (15) and (16) defined in Appendix I.

[d] Sum of the squares of differences between theoretical and observed conversions for CO_2-containing synthesis gas mixtures divided by the number of measurements n.

pies for CO_2 are lower than in Cases I and III. In all cases the adsorption heats are in the expected order $-\Delta H(CO_2) > -\Delta H(CO) > -\Delta H(H_2)$. Furthermore, the adsorption entropies have very reasonable values: $\Delta S(CO_2)$ corresponds to an entire (Cases I and III), or very substantial (Case II) loss of translational and rotational entropy of gaseous CO_2, 55.4 cal/mol-deg at 235°C, while adsorbed CO retains some 36% and adsorbed H_2 about 38% of their gas phase translational and rotational entropies of 51.6 and 36.2 cal/mol-deg, respectively (*18*). Thus adsorbed CO_2 appears rel-

TABLE 5

Values of Activation Energies of Methanol Synthesis from Carbon Monoxide, $E_a(k)$, and from Carbon Dioxide, $E_a(k')$, and Adsorption Enthalpies ΔH and Entropies ΔS Derived from the Kinetic Model Utilizing Constants in Table 4

Case I	$E_a(k) = 8.23$ kcal/mol	
	$E_a(k') = 11.28$ kcal/mol	
	$\Delta H(CO) = -19.0$ kcal/mol;	$\Delta S(CO) = -33.1$ cal/mol-deg
	$\Delta H(H_2) = -11.8$ kcal/mol;	$\Delta S(H_2) = -22.6$ cal/mol-deg
	$\Delta H(CO_2) = -30.7$ kcal/mol;	$\Delta S(CO_2) = -54.3$ cal/mol-deg
Case II	$E_a(k) = 11.74$ kcal/mol	
	$E_a(k') = 11.28$ kcal/mol	
	$\Delta H(CO) = -19.0$ kcal/mol;	$\Delta S(CO) = -33.1$ cal/mol-deg
	$\Delta H(H_2) = -11.8$ kcal/mol;	$\Delta S(H_2) = -22.6$ cal/mol-deg
	$\Delta H(CO_2) = -24.6$ kcal/mol;	$\Delta S(CO_2) = -40.3$ cal/mol-deg
Case III	$E_a(k) = 16.53$ kcal/mol	
	$E_a(k') = 11.28$ kcal/mol	
	$\Delta H(CO) = -19.0$ kcal/mol;	$\Delta S(CO) = -33.1$ cal/mol-deg
	$\Delta H(H_2) = -11.8$ kcal/mol	$\Delta S(H_2) = -22.6$ cal/mol-deg
	$\Delta H(CO_2) = -30.7$ kcal/mol;	$\Delta S(CO_2) = -55.7$ cal/mol-deg

atively strongly bound and immobile, while CO and H_2 are bonded with intermediate strength and retain some mobility in the adsorbed phase at the reaction temperature. Such a behavior is obviously favorable to the reaction in which carbon monoxide and hydrogen molecules adsorbed on different active centers must meet in a reactive collision to form the product. At the same time the strong immobile CO_2 adsorption points to the retarding effect of this gas on the synthesis in CO_2-rich synthesis gas, which is more pronounced and produces flatter plateaus on the methanol yield vs $\%CO_2$ (Fig. 2) as the temperature decreases from 250 to 225°C. The understanding of this effect is useful for the design of catalysts for CO_2-rich synthesis gases: the present model predicts that a reduction of the adsorption heat of CO_2 by only a few kilocalories while retaining the rate constant k and the oxidation potential K' should dramatically increase conversion at concentrations of CO_2 between 10 and 20%. Such a decrease of bond strength of CO_2 may be achieved by additives to the catalyst that weaken the basic character of the zinc oxide surface. Research along these lines is in progress in this laboratory and will be reported in due course.

The partial surface mobility of adsorbed CO and H_2 can best be visualized in terms of hopping of these molecules from one site to another, and it is possible to estimate the residence times τ of these reactants on the catalytically active sites from

$$\tau = \tau_0 \exp(Q/RT), \tag{19}$$

where Q is the heat of adsorption and τ_0 is defined (*19*) as

$$\tau_0 = \frac{h}{kT} \cdot f_z \cdot \frac{{}_a f_{tr}}{{}_a f_{free\ tr}} \cdot \frac{{}_a f_{rot}}{{}_g f_{rot}}. \tag{20}$$

Here, h and k are the Planck and Boltzmann constants, T is the absolute temperature, and the f's are partition functions of the adsorbed (a) or gaseous (g) molecules for rotation (rot), free translation (free tr), restricted translation (tr), and vibration normal to the surface (z). The partition function ${}_a f_{free\ tr} = 2\pi mkTA/h^2$, where A is the area available to 1 mol of adsorbate with molecular weight m. The partition functions are related to the entropies as

$$S_{rot} = (U_{rot} - U_0)/T + R \ln f_{rot} \tag{21}$$

and

$$S_{hop} = R \ln(f_{hop}/N_0). \tag{22}$$

Taking $U_{rot} - U_0 = RT$ for gas phase rotations of CO, H_2, and CO_2, the partition functions calculated from the gas phase rotational entropies of these gases at 235°C are ${}_g f_{rot}(CO) = 254.04$, ${}_g f_{rot}(H_2) = 5.86$, and ${}_g f_{rot}(CO_2) = 912.15$. The surface free-translation partition functions were calculated assuming $A = 3.2 \times 10^9$ cm^2 per mole of sites based on our earlier finding that there are some 0.16 Cu sites per ZnO unit in the catalyst (*11*, *12*), and their values are, again for 235°C, ${}_a f_{free\ tr}(CO) = 1.49 \times 10^{27}$, ${}_a f_{free\ tr}(H_2) = 1.06 \times 10^{26}$, and ${}_a f_{free\ tr}(CO_2) = 2.33 \times 10^{27}$. The partition functions for restricted rotation on the surface ${}_a f_{rot}$ were taken equal to 1, implying that rotational motion is quenched when the molecule sits on the surface site, and f_z was likewise taken equal to 1, which amounts to neglecting the small vibrational entropy. The partition functions for restricted translation ${}_a f_{tr} = f_{hop}$ were calculated from Eq. (22) using "experimental" entropies $S_{hop} = S_{tr}^{(2)}$, $S_{hop}(CO) = 51.6 - 33.1 = 18.5$ cal/mol-deg, and $S_{hop}(H_2) = 36.2 - 22.6 = 13.6$ cal/mol-deg (cf. Table 5). These values yield $f_{hop}(CO) = 6.53 \times 10^{27}$, $f_{hop}(H_2) = 5.65 \times 10^{26}$, $\tau_0(CO) = 1.64 \times 10^{-15}$ s, and $\tau_0(H_2) = 8.6 \times 10^{-14}$ s. Using "experimental" adsorption heats (Table 5) in Eq. (19), the residence times at 235°C are $\tau(CO) = 2.44 \times 10^{-7}$ s and $\tau(H_2) = 1.02 \times 10^{-8}$ s. Further examination of similar models in which the rotational degrees of freedom are not fully lost results in a range of residence times for CO between 1×10^{-7} and 2.4×10^{-7} s and for H_2 between 4×10^{-9} and 1×10^{-8} s. Cases I–III give identical results because of identical adsorption enthalpies and entro-

pies of CO and H_2. Carbon dioxide gives a range of residence times for Cases I–III; however, for all cases these times are considerably longer than those for CO and H_2.

The residence time of carbon monoxide may be compared with its reaction time to determine the probability that reaction takes place when the CO molecule is adsorbed. From an average 35.4% carbon conversion at 235°C in the $CO_2/CO/H_2$ = 6/24/70 synthesis gas (cf. Table 1) and taking 1.9×10^{14} Cu centers on 1 cm^2 of the ZnO catalyst of surface area 25 m^2/g, the turnover frequency is 0.09 s^{-1} and the reaction time is 11.1 s per conversion of one CO molecule on one site. Hence the CO molecule will hop on the surface 5×10^7 to 1.1×10^8 times before reacting. These time scales illustrate that both CO and H_2 have ample time for establishing their adsorption equilibria, a result that strongly supports the kinetic model adopted here. The adsorption of CO_2, because of its longest residence times, is the single most important factor in attaining the overall adsorption equilibrium and consequently a steady-state conversion. This has been confirmed experimentally by observing that the time required to reach a new steady state is longer when syngas composition is changed from high to lower CO_2 concentration or from low to high temperature than when the conditions are changed in the opposite direction.

Nature of the Reduced A_{red} and Oxidized A_{ox} States of the Catalyst

Although a number of specific mechanistic interpretations can be advanced to explain the redox equilibria between the catalyst and the synthesis gas, a single model will be explored wherein the CO/CO_2 ratio controls the ratio of lattice oxygen and vacancy concentrations accompanied by the corresponding distribution of the valence states of copper and zinc in the mixed catalyst.[1] The active form A_{ox} requires the catalyst to be in an oxidized state. It was established that the Cu species undergo electronic interaction with the ZnO (*12*), and such electronic interaction will participate in the formation of the reduced and oxidized states of the catalyst. Redox equilibria that may occur in this system are summarized in Eqs. (23) to (29), where the defect notation usage is that of Kofstad (*20*).

$$CO_2 + V_O^{\cdot\cdot} + 2e^- \rightleftharpoons CO + O_O \quad (23)$$

$$Cu_i^{\cdot} + e^- \rightleftharpoons Cu_i \quad (24)$$

$$Cu'_{Zn} + e^- \rightleftharpoons Cu''_{Zn} \quad (25)$$

$$Zn_i^{\cdot\cdot} + e^- \rightleftharpoons Zn_i^{\cdot} \quad (26)$$

$$Zn_i^{\cdot} + e^- \rightleftharpoons Zn_i \quad (27)$$

$$Zn_{Zn} + e^- \rightleftharpoons Zn'_{Zn} \quad (28)$$

$$2Cu + CO_2 \rightleftharpoons Cu_2O + CO \quad (29)$$

Equilibria involved in dissolution of copper in the zinc oxide phase were described

---

[1] An alternative mechanism that could qualitatively explain the maximum of the methanol synthesis rate with varying CO_2/CO ratio is one involving a formate intermediate made from carbon dioxide and hydrogen or from carbon monoxide and water. In the CO_2-free synthesis gas, the surface formate would not be formed because neither CO_2 nor H_2O are present, and consequently methanol would be formed at a low rate. In the CO_2-rich synthesis gas, the strong adsorption of CO_2 would block the sites active in formate generation, and the synthesis would be retarded as proposed in the model presented in the text. At an intermediate CO_2 concentration, the synthesis rates would be high because sufficient amounts of carbon dioxide and/or water would be available to produce the surface formate, and yet its concentration would not be high enough to block the active sites by adsorption. In this mechanism, the role of A_{ox} would be directly assumed by CO_2 or H_2O, and CO would serve only as a reservoir of carbon supplied into the surface formate by its reaction with water. However, replacement of carbon monoxide by argon in the $CO_2/CO/H_2$ = 6/24/70 vol% synthesis gas resulted in the decrease of conversion at 250°C by a factor of 17 (Table 1), although the carbon content decreased only by a factor of 5. This observation shows that methanol synthesis from carbon dioxide is a slower process than from carbon monoxide, although surface formate should be generated more readily from CO_2 and hydrogen than from CO + H_2.

earlier (*12*) and are summarized for completeness in Eqs. (30)–(32).

$$Cu_2O \rightleftharpoons Cu'_{Zn} + Cu_i^{\cdot} + O_O \quad (30)$$

$$Cu_2O \rightleftharpoons 2Cu'_{Zn} + V_O^{\cdot\cdot} + O_O \quad (31)$$

$$Cu_2O \rightleftharpoons 2Cu'_{Zn} + Zn_i^{\cdot\cdot} + O_O \quad (32)$$

Segregation of copper, which was also observed (*1*), is described by

$$Cu_i \rightleftharpoons Cu \quad (33)$$

and

$$Cu_{Zn}^{\cdot\cdot} \rightleftharpoons Cu. \quad (34)$$

In addition, zinc atoms Zn_i may move into the copper metal phase to form brass

$$Zn_i + nCu \rightleftharpoons Cu_nZn \quad (35)$$

or to the vapor phase

$$Zn_i \rightleftharpoons Zn_{(g)}. \quad (36)$$

The equilibrium constant K' used in our kinetic model is a summary equilibrium constant for all processes described by Eqs. (23)–(36).

Processes (33)–(36) may become irreversible if the copper and brass particles agglomerate and if the zinc vapor is carried away in the gas stream. The brass formation was observed on a related catalyst (*21*) but was found significant only at temperatures appreciably exceeding 250°C. The saturated vapor pressure of zinc at 250°C is 10^{-4} Torr and, in principle, evaporation by process (36) could result in a loss of the catalyst. However, all processes (33)–(36) are reversed in their initial stages by carbon dioxide reactions (23) and (29). Hence the deactivation mechanisms (33)–(36) are only serious in the absence of CO_2 or at very low concentrations of CO_2 in the synthesis gas. In our set of experiments, the activity was recovered by CO_2 even after prolonged exposure of the catalyst to CO/H_2 synthesis gas (cf. Results), and therefore the irreversible deactivation mechanisms discussed above were not operating. Of the deactivation mechanisms (33)–(36), the segregation of copper as expressed by Eqs. (33) and (34) or as induced by additional catalyst components and impurities is the most significant low-temperature deactivation mechanism.

Mechanistic Considerations

It has been demonstrated that kinetics of the type (17) accommodate mechanisms in which CO and H_2 are adsorbed on different sites as well as those in which these two reactants compete for the same sites, and hence kinetics alone do not determine the location of these two gases in the adsorbate. Given the evidence that CO is strongly adsorbed on the Cu centers in the ZnO surface (*16*), the site for hydrogen may be the ZnO surface itself as proposed originally (*2*), or the same Cu centers that bind carbon monoxide. It may well be that hydrogen is adsorbed on both the zinc oxide surface and on the Cu centers, one of the two forms being the kinetically significant species. Despite the uncertainty as to whether the CO and H_2 adsorption is competitive or not, all successful models require nearly identical adsorption energies and entropies and a constant ratio of residence times of the reactants. It is these properties that determine the relative surface coverages of CO, H_2, and CO_2. The conversion is then visualized as occurring by relatively infrequent reactive encounters resulting in extremely unstable intermediates that are rapidly converted to the product. A specific version of such a general mechanism may be one in which the hydrogen molecules slowly dissociate into surface atoms, which then immediately react with adsorbed CO and with any other partially hydrogenated species such as HCO, H_2CO, and H_3CO. Given the outlined mechanistic considerations, one can both understand the observed rapid removal of carbon from the surface during the synthesis (*2*) and foresee some difficulty in the trapping and identification of the partially hydrogenated intermediates.

Hydrogenation of Carbon Dioxide to Methanol and Methane

Carbon dioxide hydrogenations are minor pathways, as documented by its low conversion rates to methanol and methane (Table 1). The conversion to methanol may go via the reverse shift reaction,

$$CO_2 + H_2 \rightleftharpoons CO + H_2O, \qquad (37)$$

followed by hydrogenation of carbon monoxide Eq. (15). Methane, however, is formed by direct hydrogenation of CO_2 not involving reaction (37) since it is not a product from synthesis gas containing hydrogen and carbon monoxide only or with a carbon monoxide content greater than that of carbon dioxide. The conversion rates to methane are shown in Fig. 3 as a function of the CO_2 concentration and temperature. The largest amount of methane is formed at high CO_2 concentration and low temperature, indicating that *adsorbed* CO_2 is the source of methane. Bowker *et al.* (*22*) proposed that CO_2 is hydrogenated over zinc oxide to the methoxy species by the sequence

$$CO_2 \xrightarrow[e^-]{H_2} HCOO^- \xrightarrow[-H_2O]{H_2} CH_3O^- \qquad (38)$$

with a subsequent hydrogenation to methanol

$$CH_3O^- \xrightarrow[-e^-]{H_2} CH_3OH. \qquad (39)$$

Reaction (39) requires hydrogenolysis of the bond between the methoxy oxygen and an adjacent cation in the catalyst surface. We propose that the methoxy species can also undergo hydrogenolysis of the carbon–oxygen bond,

$$CH_3O^- \xrightarrow{H_2} CH_4 + HO^-, \qquad (40)$$

which constitutes a pathway to methane. Since methane formation is suppressed in the CO-rich synthesis gas, methanol synthesis from CO in the present system would not involve methoxy intermediates, if methane is formed from CO_2 by reaction (40). Thus the product composition and mechanisms involved in CO_2 hydrogenation may also shed light on the mechanism of methanol synthesis from CO. A mechanism for the latter, bypassing the methoxy route and involving formyl, hydroxycarbene, and hydroxymethyl intermediates, was proposed in our earlier work (*2*).

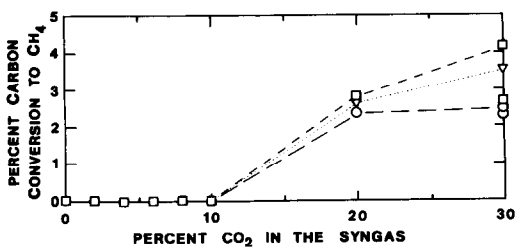

FIG. 3. The yield of methane as a function of the concentration of carbon dioxide in the synthesis gas at 225°C(□), 235°C(▽), and 250°C(○).

SUMMARY

A kinetic model that quantitatively describes the dependence of methanol synthesis on the concentration of carbon dioxide is presented herein. The maximum rate is determined by the balance between the promoting effect of CO_2, which maintains the catalyst in an active state through its oxidizing power, and the retarding effect stemming from strong adsorption of CO_2 when present in high concentrations.

It has been determined further that CO_2 is, at a slower rate than CO, hydrogenated to methanol and methane. The latter reaction constitutes a pathway specific to CO_2.

APPENDIX I

The Definitions and Values of Equilibrium Constants K_{eq} and K'_{eq}

The equilibrium constants K_{eq} and K'_{eq} are defined by their relations to the equilibrium partial pressures,

$$K_{eq} = \frac{p_{MeOH,eq}}{p^2_{H_2,eq}p_{CO,eq}} \qquad (A1)$$

and

$$K'_{eq} = \frac{p_{MeOH,eq}p_{H_2O,eq}}{p^3_{H_2O,eq}p_{CO_2,eq}}. \qquad (A2)$$

They are related to the true equilibrium constants K_p and K'_p at a total pressure of one atmosphere through the fugacity ratios K_γ and K'_γ,

$$K_{eq} = K_p/K_\gamma; \qquad K'_{eq} = K'_p/K'_\gamma. \quad \text{(A3)}$$

The K_p are functions of temperature only, while the K_γ are functions of both temperature and pressure. These p,T dependences of K_p and K_γ were taken from Refs. (*23*) and (*24*) in the form

$$K_p = 3.27 \times 10^{-13} \exp(11678/T)$$
$$K_\gamma = 1 - A_1 P \quad \text{(A4)}$$
$$A_1 = 1.95 \times 10^{-4} \exp(1703/T),$$
$$K'_p = 3.826 \times 10^{-11} \exp(6851/T)$$
$$K'_\gamma = (1 - A_1 P)(1 - A_2 P) \quad \text{(A5)}$$
$$A_2 = 4.24 \times 10^{-4} \exp(1107/T).$$

Here K'_p and K'_γ were obtained as a product of the corresponding constants for methanol synthesis from CO (A6) and the reverse shift reaction (A7), the combination of which yields methanol synthesis from CO_2 (A8).

$$CO + 2H_2 \rightleftharpoons CH_3OH \quad \text{(A6)}$$
$$CO_2 + H_2 \rightleftharpoons CO + H_2O \quad \text{(A7)}$$
$$CO_2 + 3H_2 \rightleftharpoons CH_3OH + H_2O \quad \text{(A8)}$$

The numerical values of K_{eq} and K'_{eq} entered in Table 4 result from using Eqs. (A3)–(A5) with total pressure $P = 75$ atm and the three synthesis temperatures 523, 508, and 498 K.

APPENDIX II

Algorithm for Computation of Conversion Rates Using Eq. (18)

In the computation of the integral $\int r_m dm$ in Eq. (18), incremental conversions $\Delta\alpha_{CO}$, $\Delta\alpha_{CO_2}$, and $\Delta\alpha = \Delta\alpha_{CO} + \Delta\alpha_{CO_2}$ were calculated from each increment $\Delta m \cong dm$ by the following procedure:

(1) Read-in all constants, initial flow rates of all reactants, total pressure P, and catalyst mass M;

(2) Set initial conversions equal to zero;

(3) Calculate flow rates of reactants and products from conversions α, α_{CO}, and α_{CO_2};

(4) Calculate pressures of all components from the total pressure multiplied by the ratio of their flow rates to the total flow rate;

(5) Calculate incremental conversions $\Delta\alpha_{CO}$, $\Delta\alpha_{CO_2}$, and $\Delta\alpha$ from Eq. (18), using pressures calculated sub 4 and a constant mass increment Δm. Add the $\Delta\alpha$'s and Δm to those accumulated in previous iteration cycles. If the accumulated catalyst mass reached M, store the calculated total conversions α_{CO}, α_{CO_2}, and α. In the contrary case, return to 3.

ACKNOWLEDGMENTS

This investigation was supported by U.S. Department of Energy Grants ET-78-S-01-3177, DE-AC02-80CS83001, and DE-FG22-80PC30265.

REFERENCES

1. Part III, Herman, R. G., Klier, K., and Simmons, G. W., *in* "Proc. 7th Intern. Congr. Catal." (T. Seiyama and K. Tanabe, Eds.), p. 475. Elsevier, Amsterdam, 1981.
2. Herman, R. G., Klier, K., Simmons, G. W., Finn, B. P., Bulko, J. B., and Kobylinski, T. P., *J. Catal.* **56**, 407 (1979).
3. Andrew, S. P. S., Post-Congress Symposium of the 7th Intern. Congr. Catal., Osaka, Japan, July 7, 1980.
4. Simmons, G. W., *et al.*, to be published.
5. Natta, G., *in* "Catalysis" (P. H. Emmett, Ed.), Vol. III, pp. 349–411. Reinhold, New York, 1955.
6. Denny, P. J., and Whan, D. A., *Catal., Spec. Period. Rep., Chem. Soc. London* **2**, 46 (1978).
7. Pasquon, I., and Dente, M., *J. Catal.* **1**, 508 (1962).
8. Wermann, J., Lucas, K., and Gelbin, D., *Z. Phys. Chem.* **225**, 234 (1964).
9. Bakemeier, H., Laurer, P. R., and Schroder, W., *Chem. Eng. Prog. Symp. Ser.* **66(98)**, 1 (1970).
10. Leonov, V. E., Karavaev, M. M., Tsybina, E. N., and Petrishcheva, G. S., *Kinet. Katal.* **14**, 970 (1973); Engl. trans., p. 848.
11. Mehta, S., Simmons, G. W., Klier, K., and Herman, R. G., *J. Catal.* **57**, 339 (1979).
12. Bulko, J. B., Herman, R. G., Klier, K., and Simmons, G. W., *J. Phys. Chem.* **83**, 3118 (1979).
13. Dietz, W. A., *J. Gas. Chromatogr.* **5**, 68 (1967).
14. Innes, W. B., *in* "Experimental Methods in Catalytic Research" (R. B. Anderson, Ed.), p. 84. Academic Press, New York, 1968.

15. Herman, R. G., Bulko, J. B., Parris, G., and Klier, K., 54th Colloid and Surface Science Symposium of the American Chemical Society, Bethlehem, Pa., June 15–18, 1980.
16. Parris, G. E., Ph.D. Dissertation, Lehigh University, 1981.
17. In this form the reaction is assumed to run isothermally and not to be influenced by mass transport phenomena. These requirements were nearly satisfied in our experiments, as determined by temperature distribution measurements in our reactor (the exotherms did not exceed 3 degrees) and by the flow rate dependence of the conversion in the differential reactor regime.
18. Fast, J. D., "Entropy," 2nd ed., pp. 216 and 267. Gordon and Breach, Eindhoven, 1968.
19. DeBoer, J. H., "The Dynamical Character of Adsorption," 2nd ed., p. 234. Clarendon Press, Oxford, 1968.
20. Kofstad, P., "High Temperature Oxidation of Metals," pp. 51–87. Wiley, New York, 1966.
21. Van Herwijnen, T., and DeJong, W. A., *J. Catal.* **34,** 209 (1974); **63,** 83 (1980).
22. Bowker, M., Houghton, H., and Waugh, K. C., *J. Chem. Soc., Faraday Trans. 1,* **77,** 3023 (1981).
23. Strelzoff, S., *Chem. Eng. Prog. Symp. Ser.* **66(98),** 54 (1970).
24. "Liquid Phase Methanol," Chem Systems, Inc., Report on Project No. 317, EPRI-AF-202, 1976.